Engineering Structures 179 (2019) 79–91

Contents lists available at ScienceDirect

Engineering Structures

journal homepage: www.elsevier.com/locate/engstruct

Earthquake responses of a base-isolated structure on a multi-layered soft soil foundation by using shaking table tests

Zhuang Haiyang[a,b,*], Fu Jisai[b], Yu Xu[b], Chen Su[c], Cai Xiaohui[b]

[a] School of Civil Engineering and Architecture, East China Jiaotong University, Nanchang 330013, China
[b] Institute of Geotechnical Engineering, Nanjing Tech University, Nanjing 21009, China
[c] Institute of Geophysics, China Earthquake Administration, Beijing 100124, China

ARTICLE INFO

Keywords:
Base-isolated structure
Seismic responses
Soil-structure interaction
Shaking table test

ABSTRACT

Soil-structure interaction (SSI) has a significant effect on the earthquake response of a base-isolated structure, particularly on the rotation response of the SSI system and the isolation performance of the isolation layer, as demonstrated by previous shaking table tests (Zhuang et al., 2014). On a softer soil foundation, the SSI should have a greater influence on the seismic response of an isolated structure. To this end, a new shaking table test is conducted to estimate the effect of SSI on the dynamic characteristics of a base-isolated structure on a multi-layered soil foundation including a soft clay layer. As expected, the isolation efficiency of the isolation layer is reduced by the SSI effects, especially with increasing peak ground acceleration (PGA) of the input motion. Compared with the test results for an isolated structure on a harder soil foundation, the rotation responses of the pile cap and the isolation layer in this study are stronger. Additionally, the rotation responses of the pile cap are significantly amplified by the isolation layer. This type of amplification effect can become stronger with increasing PGA of the input motion, which differs from the results for previous tests with a base-isolated structure on a harder sand foundation. Meanwhile, when the natural isolation property of the softening soil layer is considered, the seismic responses of a base-isolated structure are reduced by the SSI effects because the natural isolation of the soft soil layer can compensate for the lost isolation ability of the isolation layer.

1. Introduction

Soil-structure interactions (SSI) have complex effects on the dynamic characteristics of structures situated on soils, including base-isolated structures on soft soil [23,21]. However, conventional structural design methods neglect SSI effects, which is generally reasonable for a light structure on relatively stiff soil, e.g. low-rise buildings and simple rigid retaining walls. The effect of the SSI, however, becomes prominent for a heavy structure resting on a relatively soft soil foundation, e.g. nuclear power plants, high-rise buildings, and elevated highways on soft soil [23]. The 1995 Kobe earthquake highlighted that the seismic behaviour of a structure is strongly influenced not only by the response of the superstructure, but also by the response of the foundation and the ground [15]. Hence, the response analysis method should take into consideration the whole structural system, including the superstructure, foundation, and ground, as underlined in the Standard Specifications for Concrete Structures: Seismic Performance Verification [8].

For a base-isolated structure, the isolator should increase the natural period and effective damping ratio of the structural system. However, soft soil sediments can significantly elongate the period of seismic waves. As a result, the isolation efficiency of the isolator is reduced by the effect of the SSI [27,13]. Base-isolated structures can also resonate with long period ground vibrations [16]. Accordingly, some analytical methods have been developed to address this problem [6,17,10,13,21]. In these methods, a base-isolated structure is regarded as having a single degree of freedom, and the SSI system is modelled as an elastic soil spring and a viscous damper [28,25]. A disadvantage of these simplified methods is that the soil softening during a strong earthquake cannot be considered effectively, which affects the dynamic responses of the isolator and isolated structure.

With the rapid development of numerical modelling methods, dynamic soil-structure interactions can be investigated easily using numerical methods with a dynamic nonlinear constitutive model of the soil. These methods include the finite element method (FEM), boundary element method (BEM), and discrete element method (DEM). Using rigorous numerical analyses, Mylonakis et al. [15] have shown that the increase in the natural period of a structure due to SSI is not always

* Corresponding author.
E-mail address: zhy7802@njtech.edu.cn (H. Zhuang).

https://doi.org/10.1016/j.engstruct.2018.10.060
Received 7 April 2018; Received in revised form 20 September 2018; Accepted 22 October 2018
0141-0296/

beneficial, contrary to the suggestion of the simplified design spectra. The permanent deformation and failure of soil may further aggravate the seismic response of a structure. Sayed et al. [20] analysed the nonlinear behaviour of a base-isolated building supported on a flexible soil layer, and verified that the stiffness of the soil foundation can significantly affect the dynamic response of a base-isolated structure. Hokmabadi et al. [7] also used a fully nonlinear three-dimensional numerical model to perform a time-history analysis of the seismic response in mid-rise buildings on floating pile foundations with the effects of SSI. The results indicated that the SSI amplified the lateral deflection and inter-story drift of structures supported by floating pile foundations compared to fixed base structures.

A number of studies have examined the effect of SSI on the seismic responses of base-isolated structures. However, some of the developed methods and new findings have not been verified by the requisite model tests, and the effect of SSI on the dynamic characteristics of a base-isolated structure on soft soil has also not been investigated with an effective method. For this purpose, shaking table tests have been conducted to investigate the effect of SSI on the seismic responses of base-isolated structures [19,27,11]. In particular, the most significant finding in previous model tests is that the rotation response of the foundation can be amplified by the isolation layer, which further reduces the isolation efficiency of the isolator [27]. For a base-isolated structure on soft soil, the softening soil is expected to aggravate the rotational response of the foundation. Accordingly, this study aims to use a shaking table test to investigate the effect of SSI on the seismic responses of a base-isolated structure on a multi-layered soil that includes a soft soil layer. Based on feasible designs for the model test, the dynamic characteristics of the base-isolated structure are first compared with those of the same structure on rigid and stiff soils. Then, the respective seismic responses of the pile foundation, isolator, and isolated structure are analysed. Finally, the combined isolation of the isolator and softening soil are investigated.

2. Shaking table test design

2.1. Similitude ratio of SSI system

Standardizing the similitude ratio of physical quantities in SSI systems is very difficult when a shaking table test is used to model a seismic SSI system. However, some key physical quantities dictating the primary seismic responses of the system should be selected, and their similitude ratios should be consistent as possible [12,14]. For this purpose, the basic principles used to design the similitude ratios for the model test were as follows [27]:

1) To simulate the dynamic interaction between soil foundation and the isolated structure, the uniform similitude ratios for the physical and mechanical quantities of soil and concrete should be considered.
2) In the seismic responses of isolated structures, the aspect ratio and the first vibration mode of isolated structure should be considered in the design of the model structure.
3) The similitude ratio of lead rubber bearing should be controlled by the compressive stress to design the model lead rubber isolator.
4) For the horizontal vibration of the test system, the shear modulus of soil should be mainly considered in the similitude ratio design of soil foundation.

According to the Bukingham theory, the similitude ratios of the physical dimensions, stress, and dynamic modulus are selected and designed firstly. The similitude ratios of the physical dimensions is selected and designed according to the dimensions of the shaking table, and then the similitude ratios of the elastic modulus and density are decided according to the materials used to made the model structure and soil foundation, while the similitude ratios of other physical quantities can be deduced from their relationships with the selected quantities [27,3]. The similitude ratios of the physical quantities in these experiments are provided in Table 1.

Table 1
Similitude ratios of the model test system.

Types	Physical quantity	Similitude relationship	Similitude ratio	
			Structure	Soil
Geometric properties	Length, l	S_l	1/20	1/20
	Displacement, r	$S_x = S_l$	1/20	1/20
Material properties	Elastic modulus, E	S_E	1/4	1/4
	Equivalent density, ρ	S_ρ	20	1
	Mass, m	$S_m = S_\rho S_l^3$	1/400	1/8000
	Stress, σ	$S_\sigma = S_E S_\varepsilon$	1	1/4
	Shear modulus, G	S_G	1	1/4
Dynamic properties	Stiffness, k	$S_k = S_E S_l$	1/20	/
	Time, t	$S_t = (S_l/S_\alpha)$	1/4.47	1/4.47
	Frequency, ω	$S_f = 1/S_t$	4.47	4.47
	Acceleration, α	S_α	1	1

Note: S denotes the similitude ratio, such as S_E denotes the similitude ratio of elastic modulus E.

2.2. Isolated structure and pile foundation design

To design the model structure, a prototype isolated structure with ten stories is selected as the full-scale structure, which total height is 42 m with ten stories. The plane size of the isolated structure is 12 m × 16 m. The natural vibration frequencies of the prototype isolated structure and the corresponding non-isolated structure are about 0.41 Hz and 1.82 Hz, respectively. Under keeping the aspect ratio and the first vibration mode of the structure, a four-layer steel frame structure is designed under the assistant of the finite element analysis, which is constructed of square steel tubes as the columns and H-shaped steel beams, as shown in Fig. 1. The dimensions of the model structure are decided by the similitude ratio of the physical dimension in Table 1 and the aspect ratio of the model structure in the direction of vibration is 2.625. By the completed model test, the natural vibration frequencies of the model isolated structure and the corresponding non-isolated structure are about 2.65 Hz and 6.72 Hz (0.59 Hz and 1.50 Hz to the

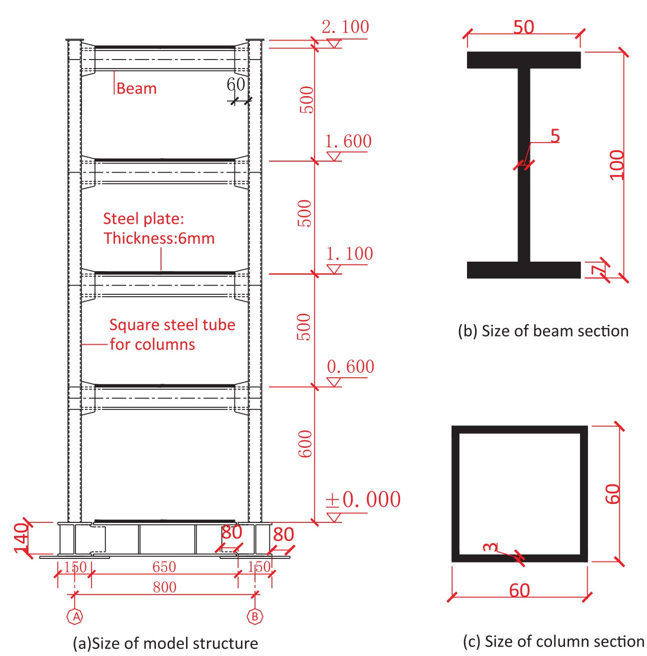

Fig. 1. Schematic of the model structure designed for the tests (units: mm).

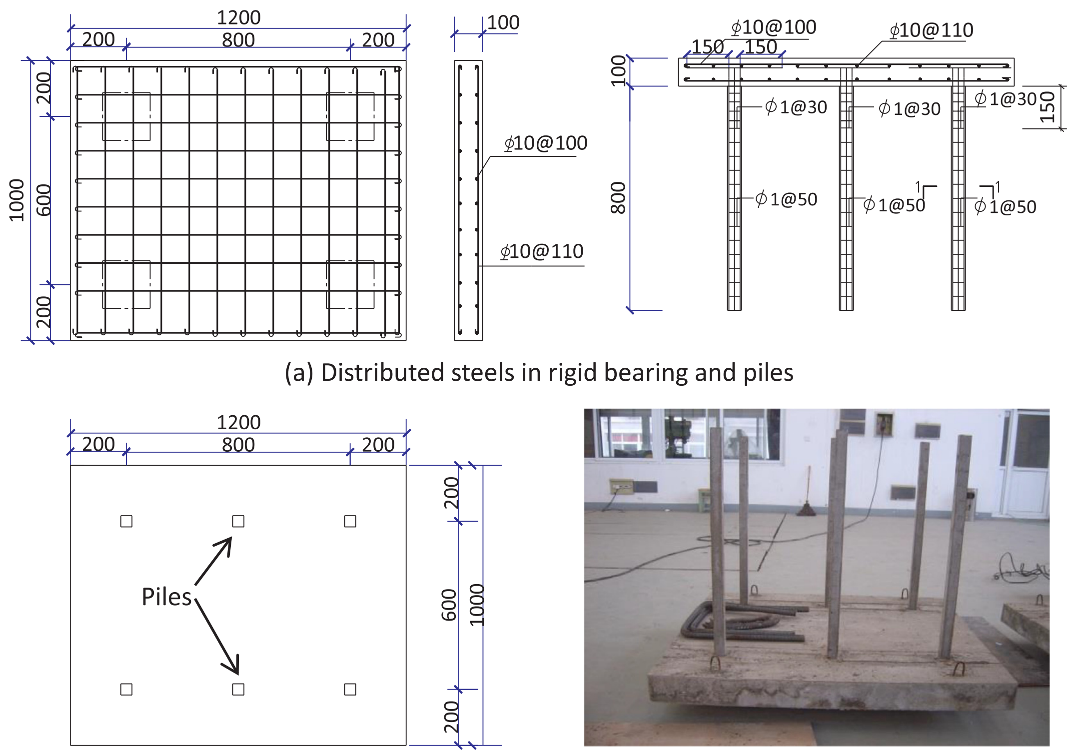

(a) Distributed steels in rigid bearing and piles

(b) Distributed piles

(c) Photo of model pile foundation

Fig. 2. Pile foundation designed for the tests (units: mm). (@ denotes the distribution distances of the steel, Φ denotes the diameter of the steel).

corresponding prototype structures according to the similitude ratio of time in Table 1), which are close to the natural vibration frequencies of the prototype isolated structure and the corresponding non-isolated structure [27]. The floor slabs are constructed of steel plates with a thickness of 6 mm. The weight of the structure model is 3.2 kN, and an additional weight of 7.36 kN is added on each floor slab to keeping the similitude ratio of the compressive stress on the lead-rubber bearing. Therefore, the total weight of the structural model with the additional weights is 40 kN. The horizontal stiffness of the model structure is approximately 1.5 kN/mm, and its viscous damping is approximately 13.5 kN·s/m [27].

A pile foundation is designed as a reinforced foundation for the base-isolated structure. The pile cap is a rigid block with dimensions of 1.2 m (vibration direction) × 1.0 m (vertical to the vibration direction) × 0.1 m (thickness). The pile foundation consists of six piles which each have a cross section of 0.035 m × 0.035 m. Micro concrete and zinc-coated steel wires are used to construct the pile foundation, and the pile foundation model and distribution of the reinforced rebar are shown in Fig. 2.

To the prototype isolated structure, the transection diameter of the lead-rubber bearings is 600 mm and the total thickness of the rubber layers is 120 mm. According to the parameters of prototype bearing offered by the manufacturer, the characteristic parameters of isolators are shown in Table 2. However, it is very difficult to design the model bearings fully according to the similitude ratios as shown in Table 1. By considering the total weight of model isolated structure and the isolation performance of the model bearing, six lead-rubber bearings are constructed with a transection diameter of 100 mm and an average compressive stress of 1.3 N/mm^2. The physical properties of the model lead-rubber bearing are given in Table 3 as determined by load-shear tests. The mechanical properties of the model isolators are provided in Table 4. Four model isolators (No. 1, No. 2, No. 5, and No. 6) which have similar mechanical properties are selected and used to support the upper model structure. A model lead-rubber bearing is shown in Fig. 3.

Table 2
Physical and mechanical properties of the prototype lead-rubber bearings.

Physical quantity	Value	Physical quantity	Value
Shear modulus of rubber, G (N/mm^2)	0.4	First form factor, S_1	25.5
Bulk modulus of rubber, E_b (N/mm^2)	2000	Second form factor, S_2	5.0
Yield load, Q_y (kN)	94.2	Diameter of pencil lead (mm)	120
Damping, (kN·s/m)	14.7	Diameter of bearing (mm)	600
Pre-yield stiffness $k_{y,0}$ (kN/mm)	6.519	Post- yield stiffness $k_{y,50}$ (kN/mm)	1.033

Table 3
Physical properties of the model lead-rubber bearings.

Physical quantity	Value	Physical quantity	Value
Shear modulus of rubber, G (N/mm^2)	0.6	First form factor, S_1	19.2
Bulk modulus of rubber, E_b (N/mm^2)	1960	Second form factor, S_2	3.48
Yield load, Q_y (kN)	0.44	Diameter of pencil lead (mm)	8
Damping, (kN·s/m)	10.93	Diameter of bearing (mm)	100

Detailed design of the model structure and lead-rubber bearings were introduced by Zhuang et al. [27].

Force-displacement loops for the model lead-rubber bearings during tests are shown in Fig. 4, and demonstrate the performance of the model lead-rubber bearings. It should be explained that the loops shown in Fig. 4 are for a single isolator, which is recorded by a specialist force sensors shown as following Fig. 6. The results verify that the model lead-rubber bearings all perform excellently during the tests. The force-displacement loops in this test are also compared with those from a previous test with a base-isolated structure on a rigid

Table 4
Mechanical properties of the model lead-rubber bearings by the tests.

Test sample No.	Vertical stiffness k_v (kN/mm)		Horizontal yield stiffness k_y (kN/mm)		Yield load Q_y (kN)	
	σ_v = 5 MPa	σ_v = 10 MPa	σ_v = 10 MPa		σ_v = 10 MPa	
			γ = 50%	γ = 100%	γ = 50%	γ = 100%
1	232.8	253.5	0.201	0.164	0.492	0.577
2	242.5	249.1	0.207	0.161	0.481	0.566
3	250.7	263.5	0.215	0.171	0.511	0.613
4	227.1	236.2	0.192	0.154	0.453	0.549
5	238.6	249.1	0.201	0.159	0.481	0.589
6	236.2	243.6	0.199	0.161	0.472	0.577
Average	237.9	249.2	0.203	0.16	0.482	0.578
R	8.1	9.2	0.008	0.006	0.019	0.0216

Note: σ_v is the vertical stress loaded on the rubber bearings during the tests, R is the standard deviation, and γ is the magnitude of shear strain for the model rubber bearings during the tests.

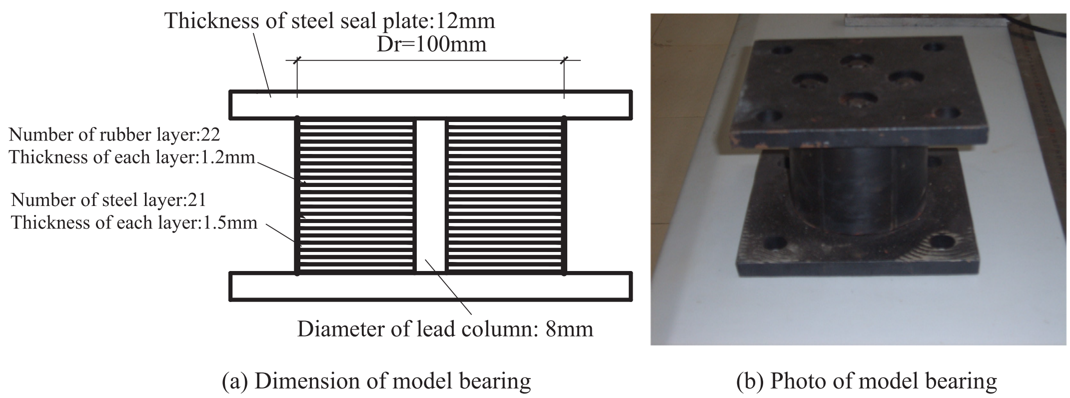

Fig. 3. Model lead-rubber bearing used in these tests.

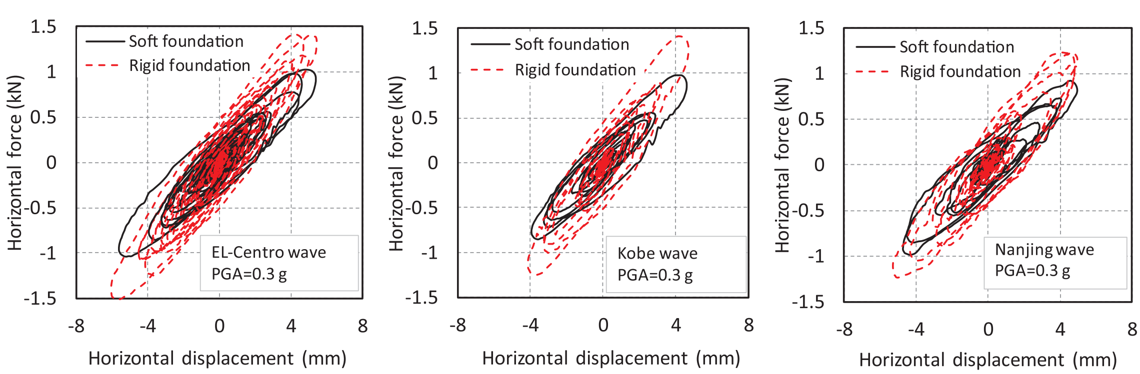

Fig. 4. Force-displacement loops of the model lead-rubber bearings during different tests.

foundation. The results show that the horizontal stiffness of the model lead-rubber bearing is lower on a soft soil than on rigid ground. It has been shown that the horizontal stiffness of a lead-rubber bearing decreases when the vibration frequency of the input motion decreases [26]. As a result, softening soils can also filter the high frequency vibrations of the input motion, which is consistent with results for the effect of the input vibration frequency on the horizontal stiffness of a lead-rubber bearing [26].

2.3. Multi-layered soil design

In the first design of the soil, a 60 cm thick bottom dense sand layer and a 70 cm thick upper soft clay layer were used to make up the soil. When the model structure and additional weight were loaded onto the pile foundation, the soil ground was damaged so severely that the pile foundation settled onto the bottom of the soil. As a result, the shaking table test had to be suspended. To solve this problem, the model soil foundation was redesigned with three soil layers, including a 30 cm thick upper dense sand layer, a 40 cm thick middle soft clay layer, and a 60 cm thick bottom dense sand layer, as shown in Fig. 5. The bottom sand layer is compacted by the stratified compaction method to prevent liquefaction, after which water is added into the soil box to saturate the sand. After one day, the sun-dried clay is crushed into a powder, placed on a steel wire sieve, and then added slowly to the water in the test box to guarantee the foundation is homogeneous. After standing for 2 days, the excess water is removed from the test box, and the top sand layer is added by the stratified compaction method. After one day, the model pile foundation is compressed into the soil, and the upper isolated structure is then fixed on the pile bearing. Finally, the shaking table test is begun after one more day. Photos taken during the tests are shown in Fig. 5. For reducing the effect of each test on the consistency of soil condition, the subsequent test should begin after about one hour so that

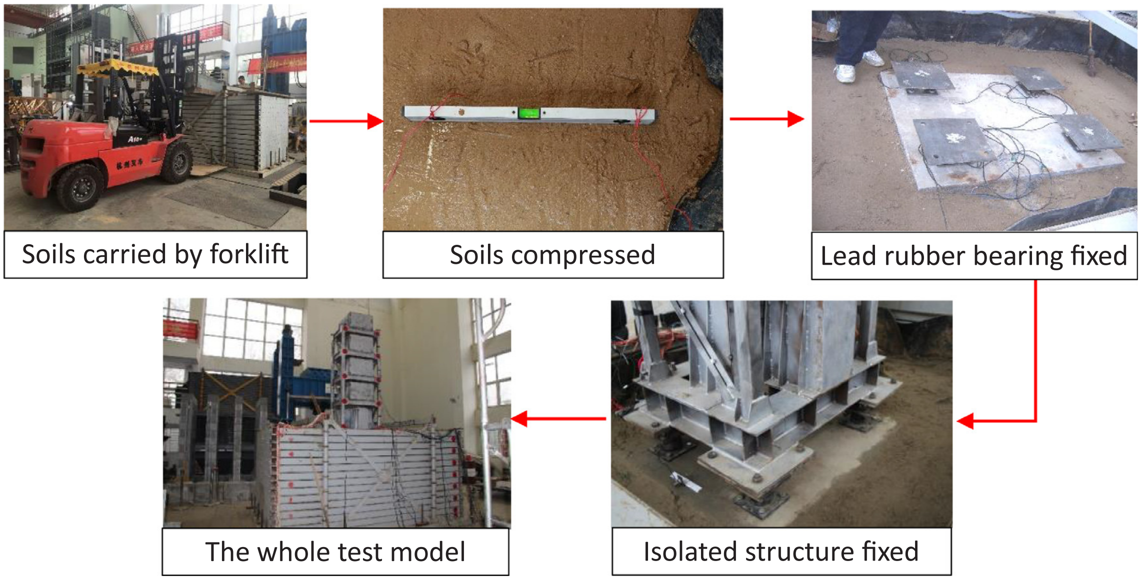

Fig. 5. Photos taken during construction of the soil foundation.

Table 5
Physical and mechanical parameters of the model soil layers.

Soil layer	Thickness (m)	Density, ρ (g/cm^3)	Shear modulus, G (MPa)	Friction angle (°)
Top sand layer	0.3	1.76	11.3	27
Soft clay	0.4	1.93	3.91	18
Bottom sand layer	0.6	1.92	27.6	28

the accumulated pore water pressure can dissipate.

For the model soil under a small confining effective stress, its dynamic properties have been tested by the resonant-column test in the previous model tests [27]. Meanwhile, the physical condition of the model soil ground has also been evaluated by measuring the wave propagation velocity of the model foundation [29]. By the test results, the similitude ratio of shear modulus can be deduced to be about 1/4 according to the confining effective stress of soil ground. The physical parameters of the soil were also tested, and are listed in Table 5.

The laminar shear box used in this test consists of 15 rectangular plane steel frames, each welded to four square steel tubes. Grooves with steel balls are fixed between the frame layers to form freely horizontal-sliding supports [27]. The internal clearance size of this test box is approximately 3.5 m (vibration direction) × 2.0 m (vertical to the vibration direction) × 1.7 m (height). This test box has been shown to efficiently reduce boundary effects [2].

Accelerometers (Nos. A1–A17) are arranged on each floor of the isolated structure and in the soil to record the horizontal acceleration responses of the SSI system. Additional accelerometers (Nos. V1–V4)

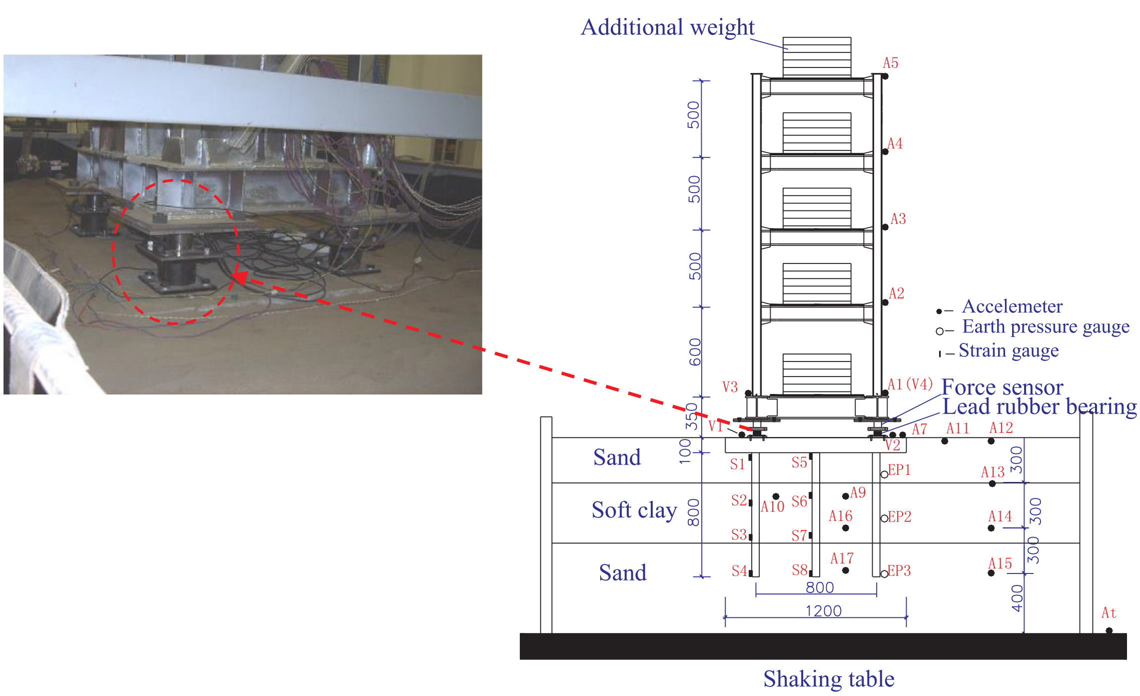

Fig. 6. Arrangement of sensors in the model SSI system.

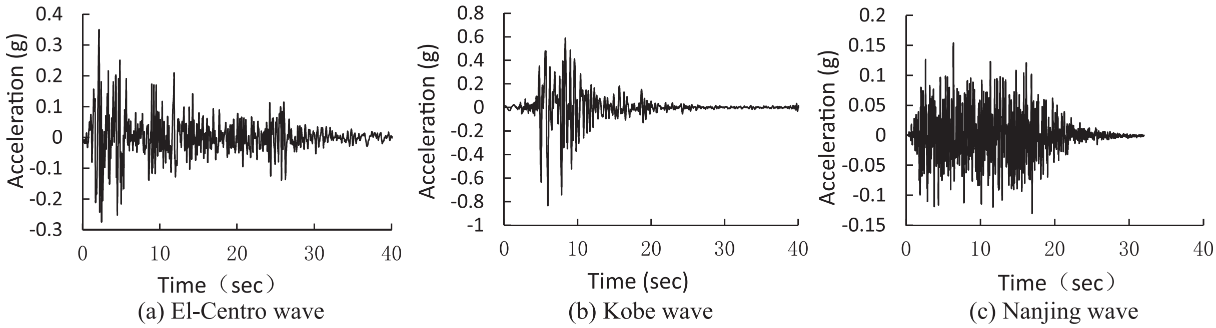

Fig. 7. Original time-histories of the earthquake waves used as input motions.

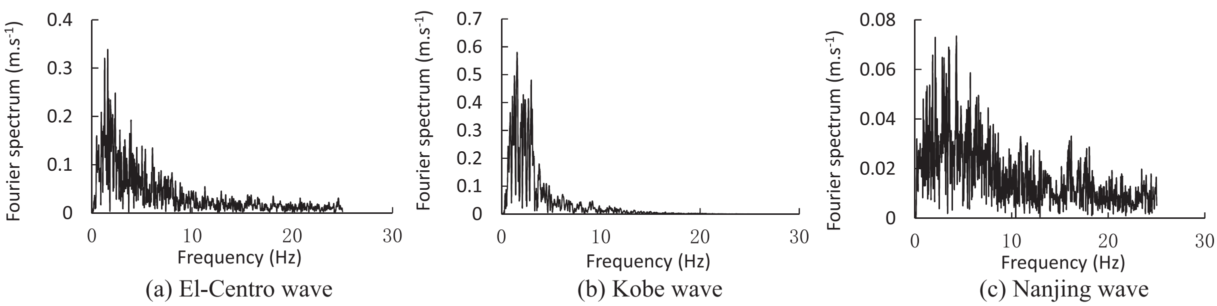

Fig. 8. Fourier spectra of the accelerations used as input motions.

Table 6
Load methods for the shaking table test.

Group No.	Load No.	Ground motion	Designed PGA (g)	Actual PGA (g)
–	WN1	White noise	0.05	—
1	El1	El-Centro	0.05	0.068
	NJ1	Nanjing	0.05	0.072
	KB1	Kobe	0.05	0.065
2	EL2	El-Centro	0.15	0.204
	NJ2	Nanjing	0.15	0.133
	KB2	Kobe	0.15	0.206
3	EL3l	El-Centro	0.3	0.327
	NJ3	Nanjing	0.3	0.260
	KB3	Kobe	0.3	0.308
4	KB4	Kobe	0.5	0.391
–	WN2	White noise	0.05	—

are also arranged on the pile cap and the top plate of the isolation layer to record the vertical acceleration responses. Strain gauges (Nos. S1–S6) are attached to the piles to record their strain responses. The arrangement of sensors in the tests are shown in Fig. 6. Before an accelerometer is arranged in the soils, which should be fixed in a small box, and then the small box is filled by the transparent silicon. In this way, the equivalent density of the box with an accelerometer is reduced to be close to the surrounding soil such that they could have consistent motions with the surrounding soils [29].

2.4. Loading conditions

The El-Centro earthquake wave (El wave), Kobe earthquake wave (KB wave), and Nanjing artificial earthquake wave (NJ wave) are used as input motions. The El wave was recorded during the Imperial Valley earthquake of 1940, with an original peak ground acceleration (PGA) of 0.349 g. The duration of this strong earthquake was 26 s. The KB wave was recorded by the Marine Meteorological Station during the Kobe earthquake of 1995, with an original PGA of 0.85 g and a duration of approximately 10 s. The NJ wave was calculated by the software COMPSYN, and was compiled by the Institute of Engineering Mechanics (IEM) of the China Earthquake Administration. Its original peak acceleration was 0.15 g, and the duration of this strong earthquake was 20 s. The three earthquake waves and their Fourier spectra are shown in Fig. 7 and Fig. 8, respectively. The time increment of the original ground motion is 0.02 s.

The Fourier spectra show that the primary frequency bandwidth of the KB wave is the smallest, while that of the NJ wave is the largest. The Kobe wave is a near-field ground motion, while the Nanjing wave is a far-field ground motion, and the El-Centro wave is a mid-far-field ground motion. According to the similitude ratio for time, the time increment of the input motion is adjusted to 0.0045 s, and the PGA is adjusted to the values given in Table 6. However, the PGAs recorded on the shaking table are not equal to the designed value in each test.

Table 7
Fundamental vibration frequency and damping ratio of the base-isolated structure.

Test condition	Type of foundation									
	Rigid foundation				Stiff soil				Soft soil	
	Frequency (Hz)		Damping ratio (%)		Frequency (Hz)		Damping ratio (%)		Frequency (Hz)	Damping ratio (%)
Isolated	Yes	No	Yes	No	Yes	No	Yes	No	Yes	Yes
Before test	2.65	6.72	8.3	3.0	2.48	4.36	10.5	9.7	2.4	14.8
After test	2.62	6.12	8.8	4.9	2.31	4.2	17.2	12.2	2.27	18.4

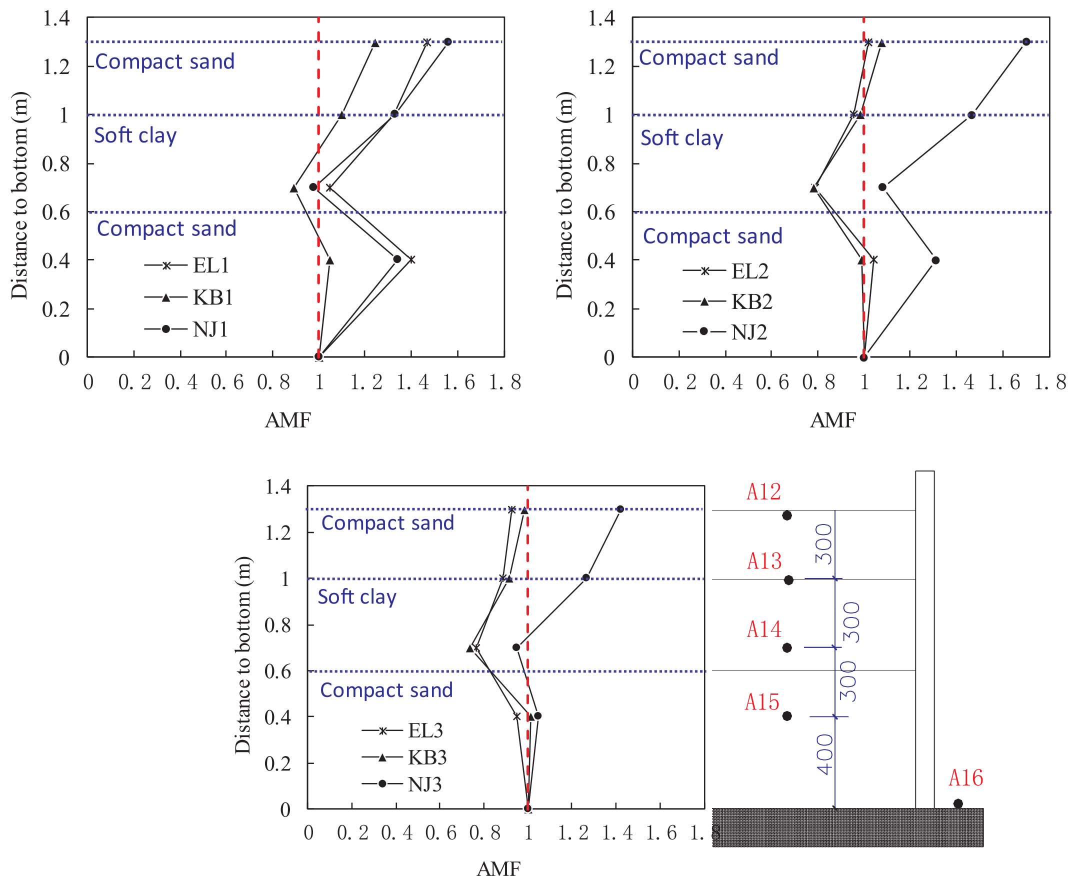

Fig. 9. Amplification magnification factor (AMF) under different input motions.

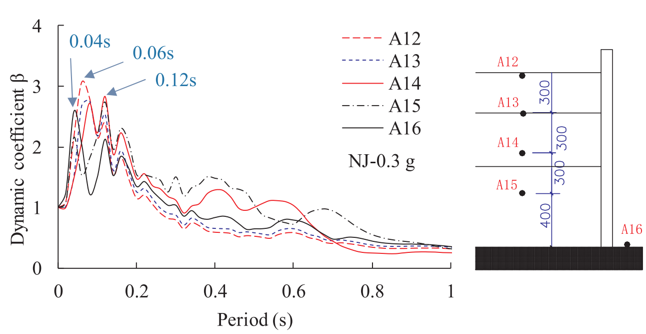

Fig. 10. Normalized response acceleration spectra under the Nanjing wave input motion.

Accordingly, the actual PGAs at the shaking table for each vibration are also provided in Table 5.

3. Analysis of test results

3.1. Dynamic characteristics of the isolated structure

The fundamental vibration frequency and damping ratio of the SSI system can be deduced from the dynamic response of the isolated structure with input white noise [4]. These are also compared with results for the isolated structure and non-isolated structure on a rigid foundation or a stiffer soil in previous tests. The test results demonstrate that SSI greatly affects the dynamic characteristics of a base-isolated or a non-isolated structure. Firstly, the results in Table 7 indicate that the fundamental vibration frequencies with the SSI effect are notably smaller than those without an SSI effect whether the structure is isolated or not. To the non-isolated structure, the SSI effect should be more greatly, which fundamental vibration frequency is reduced about 35.1% by the SSI effect. The fundamental vibration frequency of the base-isolated structure was only reduced about 6.4% by the stiff soil foundation and 9.1% by the soft soil foundation, respectively. To the base-isolated structure on soil foundation, the type of soil foundation has little effect on its fundamental vibration frequency. In addition, the results in Table 7 also indicate that the damping ratio of the SSI system is larger than that of the base-isolated structure on a rigid foundation, especially for the damping ratio of the non-isolated structure increasing from 3.0% to 9.7%. To the base-isolated structure on stiff soil foundation, the damping ratio of SSI system is about 1.27 times that of the base-isolated structure on rigid foundation. However, the type of soil foundation also has great effect on the damping ratio of the SSI system, which increases from 10.5% on stiff soil foundation to 14.8% on soft soil foundation. Accordingly, the SSI effect greatly affects the dynamic characteristics of a non-isolated structure, largely because the soil filters the high-frequency vibrations of the input ground motion. In terms of the stiffness of the soil, a softer multi-layered soil should slightly reduce the fundamental vibration frequency of the base-isolated structure on a stiffer soil but greatly increased the damping ratio of the SSI system.

3.2. Seismic response of the soil

The seismic response of the soil is very important for the model tests in this study, and are crucial to the success of these tests. Fig. 9 shows the acceleration magnification factor (AMF) of the model soil. Here, the AMF is defined as the PGA of the response acceleration of the soil divided by the PGA of the input motion at the shaking table. Generally, the spectrum characteristics of the input motion greatly influence the seismic response of soft soils. When the PGA of the input motion is very small (as in test group No. 1), the AMFs of the soil under the Kobe wave

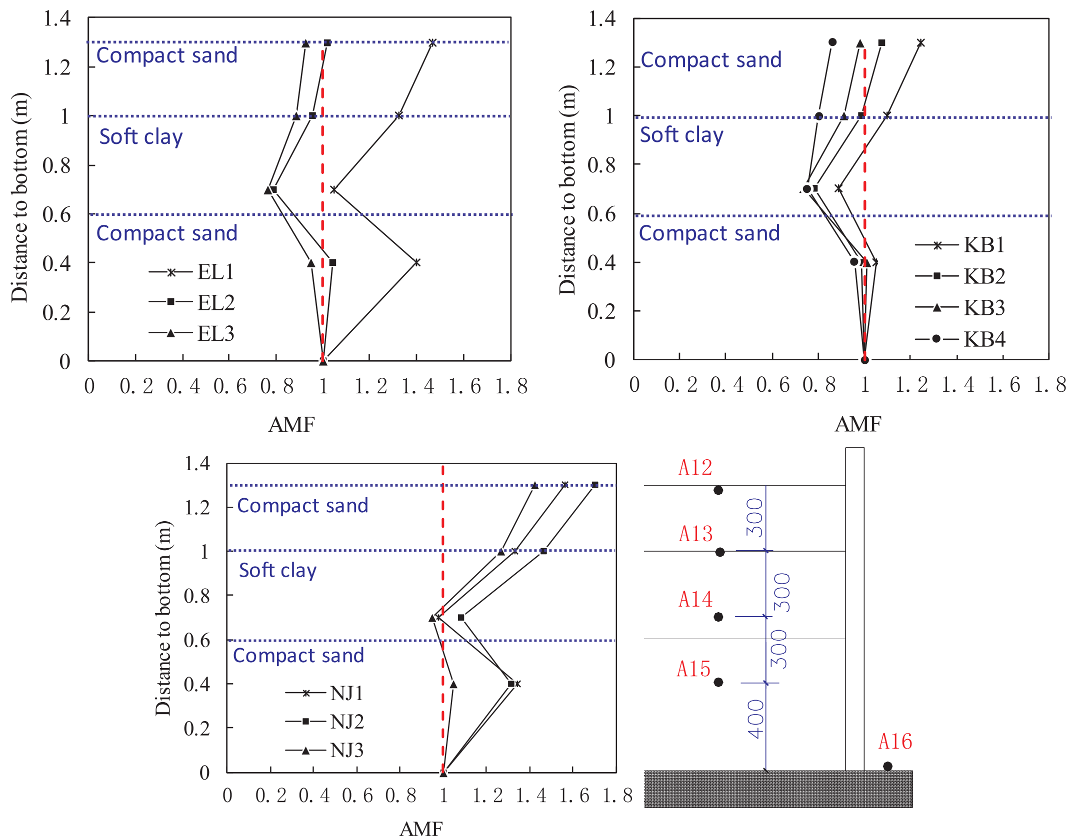

Fig. 11. Amplification magnification factor (AMF) under different input motion PGA.

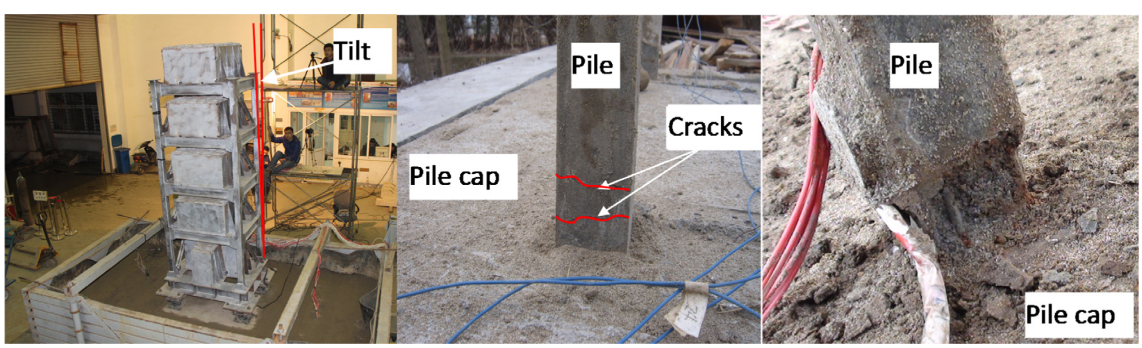

(a) Tilt of isolated structure (b) Cracks at the top end of the pile (c) Exposed steel

Fig. 12. Damage to the pile and tilt of the isolated structure after testing.

Table 8
PGAs at the top of the pile cap (No. A7) and the top plate of the isolation layer (No. A1).

Test group	Location	Kobe motion		El-Centro motion		Nanjing motion	
		PGA ($m{\cdot}s^{-2}$)	A1/A7 (%)	PGA ($m{\cdot}s^{-2}$)	A1/A7 (%)	PGA ($m{\cdot}s^{-2}$)	A1/A7 (%)
1	A1 A7	0.175 0.490	64.6	0.355 0.669	46.9	0.473 0.703	64.2
2	A1 A7	1.101 2.160	50.3	1.048 1.998	47.5	0.725 1.430	50.7
3	A1 A7	1.629 3.026	45.8	2.286 2.94	22.3	1.616 2.94	45.0
4	A1 A7	2.572 3.827	32.8	– –	–	– –	–

motion is close to that under the Nanjing wave motion, which are both larger than that under El-Centro wave motion. However, as the PGA of the input motion increases in test group Nos. 2 and 3, the AMFs of the soil foundation under the Kobe wave motion are close to those under the El-Centro wave motion, which are both smaller than that under the Nanjing wave motion.

In the above results, the low frequency vibration of the Nanjing wave motion is much stronger than that of the other two motions (Fig. 8), which is the primary reason for the observed difference in seismic responses of the model soil foundation. In other words, the low-frequency vibration of the Nanjing wave motion is amplified significantly by the softening soil layer under the large PGA of the input motions in test group Nos. 2 and 3, as shown in Fig. 10 (Dynamic coefficient b is the normalized acceleration responses spectra). At the same time, the predominant period of the softening soil should increase. As a result, the seismic responses of the soil are strongest under the Nanjing wave input motion in test group Nos. 2 and 3.

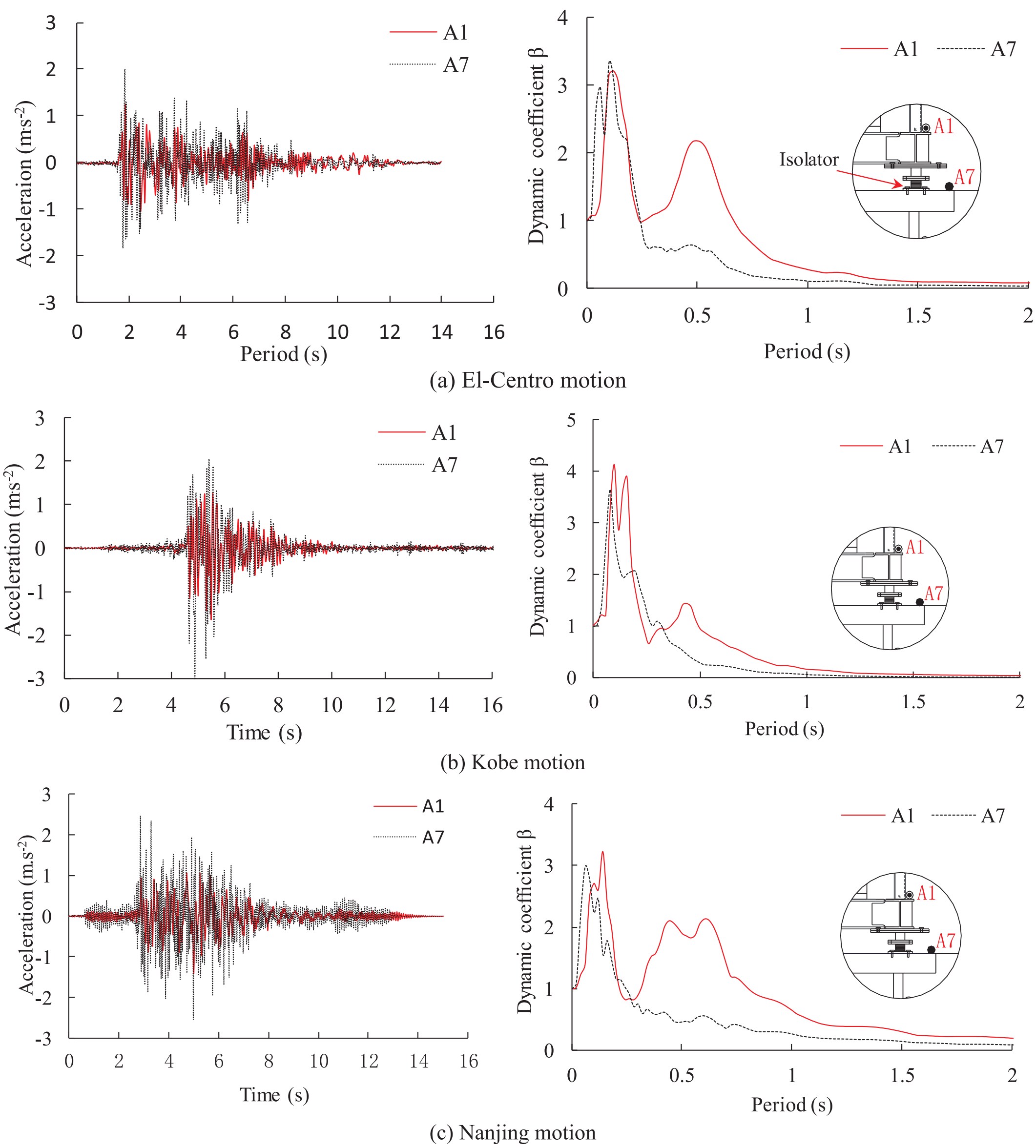

Fig. 13. Acceleration responses of the isolation layer for test group No. 3.

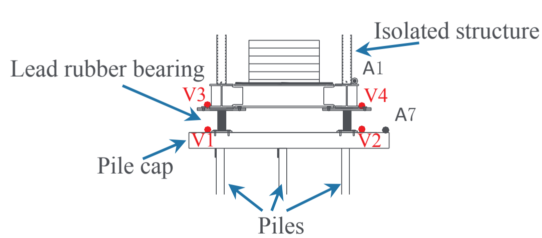

Fig. 14. Accelerometers fixed at the top of the pile cap and the isolation layer.

Fig. 11 shows the effect of the PGA of the input motion on the AMF of the model soil. Generally, the AMFs on the ground surface decrease with increasing PGAs for the Kobe or El-Centro input motions. However, the AMF on the ground surface initially increases and then decreases with increasing PGA of the Nanjing input motion. In this study, the ways in which the spectrum of the input motion affect the AMFs at the ground surface cannot be determined. Fig. 11 shows that the PGA of the input motion appear to be amplified by the bottom sand layer, but the AMFs in sand layer appear to decrease with increasing PGA for each input motion. However, at the bottom of the soft clay layer, the PGAs are all reduced. The acceleration responses are then continuously amplified by the upper soft clay layer and the upper sand layer. According to existing studies on the seismic responses of a soft free-field [1], the observed trends in the AMFs of the model soft soil in this study are generally similar to the seismic response laws of an actual multi-layered free field that includes a soft soil layer.

Table 9
Peak angular accelerations of the pile foundation and the isolation layer.

Input motion	Loading No.	$\theta''_{1,max}$(rad·s^{-2})	$\theta''_{2,max}$(rad·s^{-2})	$\theta''_{2,max}/\theta''_{1,max}$
El-Centro	EL1	0.347	0.418	1.20
	EL2	0.821	1.762	2.15
	EL3	1.165	2.652	2.28
Kobe	KB1	0. 414	0. 432	1.04
	KB2	0.810	0.911	1.12
	KB3	0.960	1.129	1.18
	KB4	1.289	2.326	1.81
Nanjing	NJ1	0.356	0.435	1.22
	NJ2	0.556	0.659	1.19
	NJ3	0.940	0.920	0.98

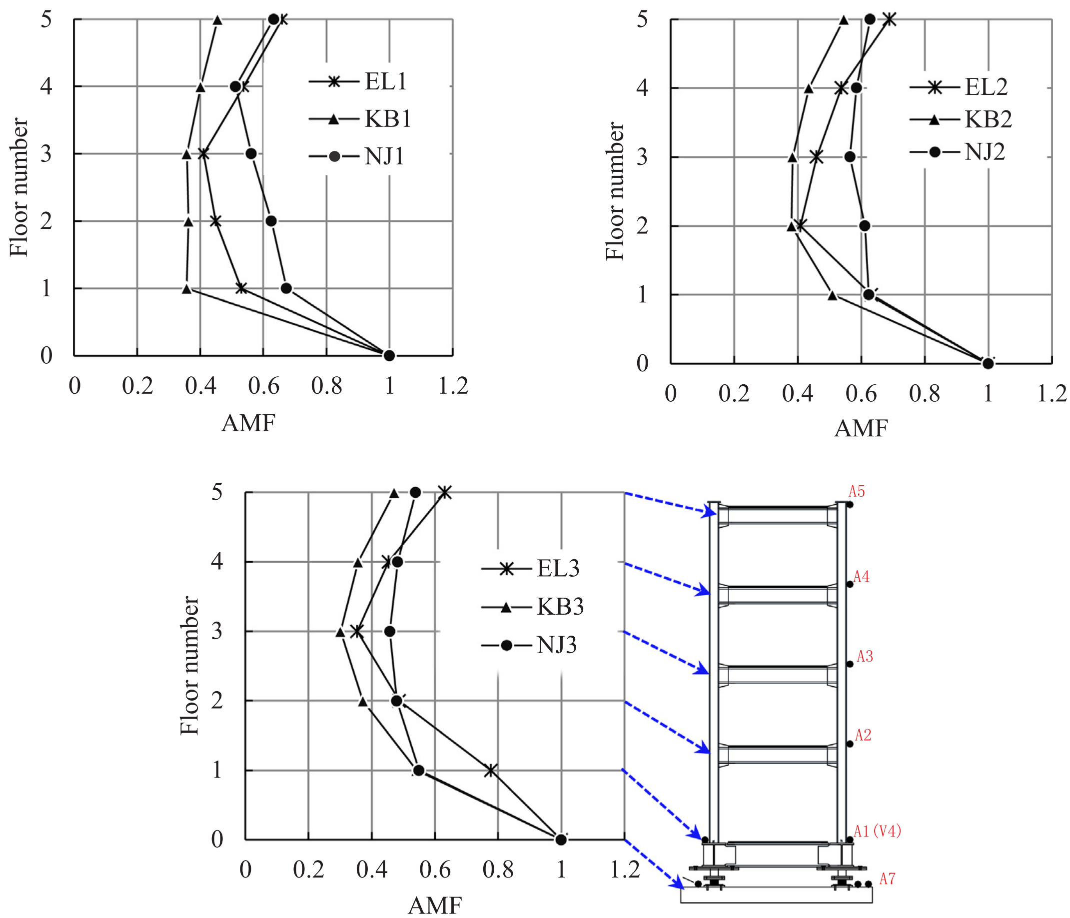

Fig. 15. AMFs of the isolated structure under different input motions.

At the end of the test, the isolated structure has an obvious incline, as shown in Fig. 12(a). Some cracks are also observed near the top end of the piles, as shown in Fig. 12(b). In particular, the concrete at the top end of a pile is crushed and the steel is exposed, as shown in Fig. 12(c).

3.3. Seismic responses of the isolation layer

The PGA at the top of the pile cap (No. A7) is compared with that at the top plate of the isolation layer (No. A1) to investigate the seismic responses of the isolation layer, and the results are summarized in Table 8. The ratio between the PGA at the top plate of the isolation layer and that at the top of the pile cap generally decreases as the PGA of the input motion increases, which means that the isolation efficiency of the isolation layer also decreases as the PGA of the input motion increases. This was also observed in previous model tests with an isolated structure on a stiffer soil foundation [27]. Fig. 13 shows the acceleration responses of the isolation layer for test group No. 3. The high-frequency vibrations are reduced, while the low-frequency vibrations are simultaneously significantly amplified by the isolation layer. This result agrees with the essential seismic property of the isolation layer, and also confirms that the isolation layer is in working order.

Rotation of the isolation layer is not considered when the isolated structure is fixed on a rigid foundation. However, previous earthquake damage shows that rotation of the foundation significantly affects the seismic response of the upper isolated structure [24]. Accordingly, to investigate the rotation response of the isolation layer, two accelerometers (No. V1 and No. V2) are fixed symmetrically at the top of the pile cap to measure the vertical acceleration, while two accelerometers (No. V3 and No. V4) are fixed at the top plate of the isolation layer, as shown in Fig. 14. According to the method proposed by Chen et al. [5], the rotation angular acceleration of the pile cap (θ_1'') and the rotation angular acceleration of the isolation layer (θ_2'') can be calculated as follows:

$$\theta_1'' = \frac{V_1 + V_2}{L_1} \tag{1}$$

$$\theta_2'' = \frac{V_3 + V_4}{L_2} \tag{2}$$

where V_1, V_2, V_3, and V_4 are the vertical peak accelerations recorded by accelerometer Nos. V1, V2, V3, and V4, respectively (Fig. 14); L_1 is the horizontal distance between accelerometer No. V1 and No. V2; and L_2 is the horizontal distance between accelerometer No. V3 and No. V4.

The peak angular accelerations (PAA) are calculated with Eqs. (1) and (2), and the results are given in Table 9. The PAAs of the pile cap and isolation layer all generally increase as the PGA of the input motion increases. The PAAs of the pile cap, which range from 0.347 to 1.129 rad·s^{-2} in this test, are much larger than those in a previous model test with a stiffer soil foundation, which ranged from 0.062 to 0.355 rad·s^{-2} [27]. This result indicates that the soft soil layer strongly influenced the rotation response of the pile cap. Meanwhile, the PAAs of the isolation layer are also much larger than those of the pile cap, indicating that the rotation response of the pile cap is significantly amplified by the isolation layer. This amplification also becomes stronger as the PGA of the input motion increases for the Kobe motion or El-Centro motion inputs. However, the amplification effect of the isolation layer weakens slightly with increasing PGA of the input motion for the Nanjing motion input.

In tests with an isolated structure on a stiffer soil foundation [27], the rotation responses of the pile cap and isolation layer all weaken with increasing PGA of the input motion, while the rotation-

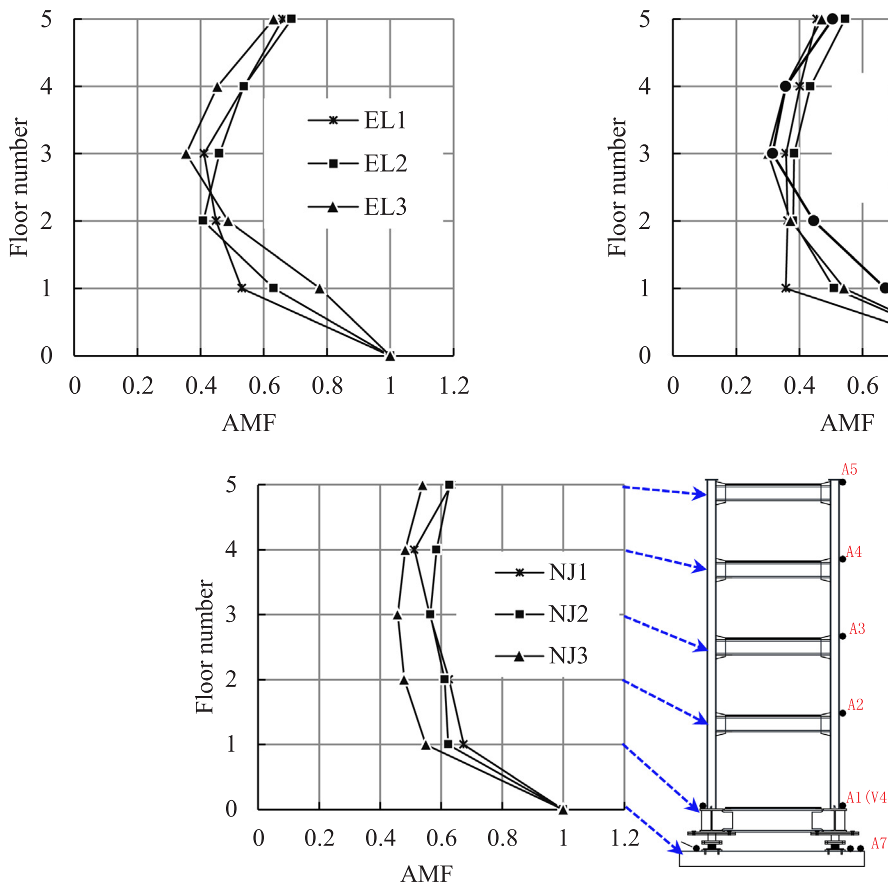

Fig. 16. AMFs of the isolated structure under different input motion intensities.

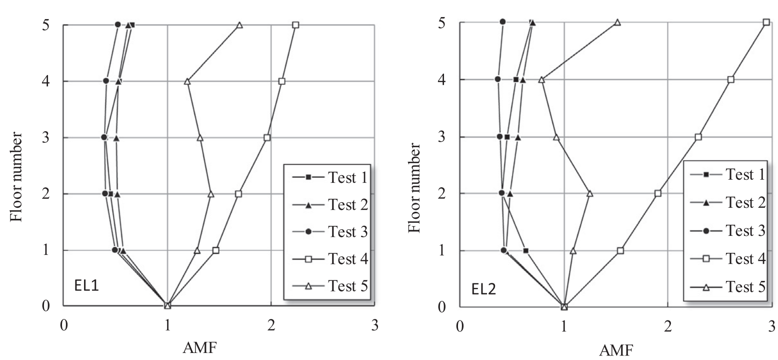

Test	Conditions
1	Soft, Base-isolated
2	Stiff , Base-isolated
3	Rigid, Base-isolated
4	Rigid, Non-isolated
5	Stiff , Non-isolated

Fig. 17. AMFs of the base-isolated and non-isolated structures on different foundations.

amplification effect of the isolation layer reduces as the PGA of the input motion increases, which is different from the results of the current test. This difference can be explained by the different soils. The model soil in the previous test by Zhuang et al. [27] only consists of a sand layer. After each input motion, the sand was compacted, which increases the stiffness of the soil. However, repeated input vibrations have little effect on the stiffness of a soft clay layer. On the contrary, the soil layer in this study will be softened by stronger input motions.

3.4. Seismic responses of the isolated structure

The AMFs of the base-isolated structure are shown in Fig. 15. The results demonstrate that the spectra properties of the input motions significantly influence the seismic responses of the base-isolated structure. However, this effect reduces as the PGA of the input motion increases. Similar to the analysis in Section 3.2, the amplified low frequency vibrations of the input motion intensify the seismic responses of the isolated structure, which also suggests that the isolation efficiency of the isolation layer is reduced. Thus, the isolation efficiency of the isolation layer is lowest when the input motion is the Nanjing wave, and is highest when the Kobe wave is used as the input. Meanwhile, according to Fig. 13, the acceleration responses at the bottom of the isolation layer are greatly amplified by the isolation layer at a period of approximately 0.5 s, which is very close to the natural vibration period of the isolated structure (0.42 s). In terms of input motion, the amplification of the acceleration response near 0.5 s is the strongest when the Nanjing wave is used as the input, and it is weakest when the Kobe wave is input. Accordingly, the acceleration responses of the isolated structure are also strongest when the Nanjing wave is input, and are weakest when the Kobe wave is input.

Generally, the seismic responses at the middle floors of the isolated structure are smaller than those of the top or bottom floors, which is

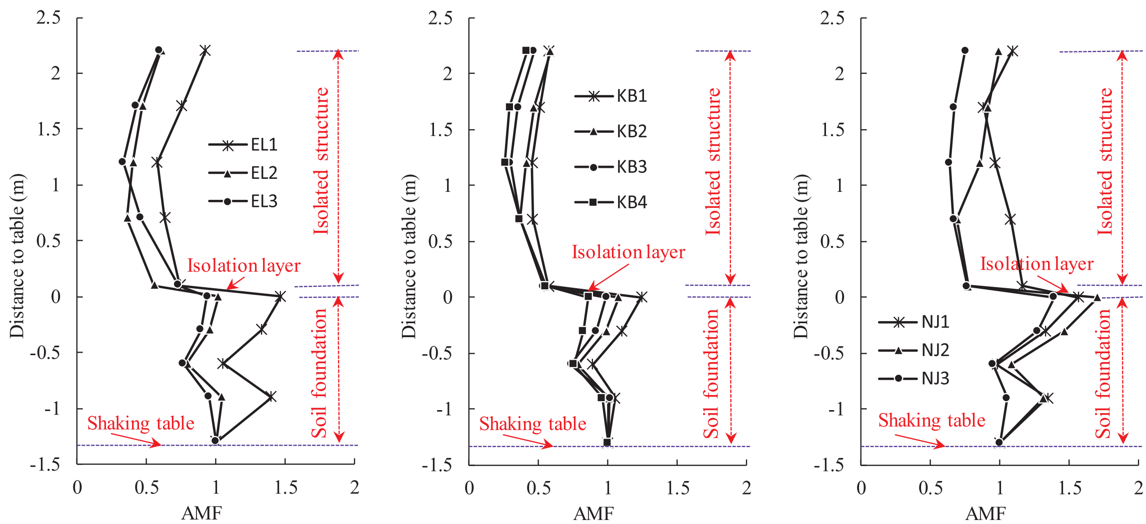

Fig. 18. AMFs of the soil-isolated structure interaction system.

similar to the seismic responses observed for a base-isolated structure on a rigid foundation or on a stiffer soil [27]. The AMFs of the base-isolated structure are also compared at varying input motion PGA in Fig. 16. The results indicate that the PGA of the input motion mainly changes the floor at which the smallest AMF occurs.

Fig. 17 shows the effect of SSI on the AMFs of the base-isolated and non-isolated structure. It affirmatively proves that the soil foundation should reduce the isolation efficiency of the isolation layer, especially for the soft soil foundation in Load No. EL2, and the AMF at floor number No. 1 of the isolated structure on soft soil foundation is about 1.47 times of that on rigid foundation and about 1.65 times of that at the top of the isolated structure. At the same time, the AMFs of the isolated structure on soil foundation are all larger than those of the isolated structure on the rigid foundation. For the two soil foundations, the acceleration responses at the upper floors of the isolated structure are amplified greatly. To a non-isolated structure on a soil foundation, SSI has strongly reduced its seismic response, and this kind of effect also becomes stronger and stronger from floor number No. 1 (isolation layer) to No. 4, and the AMF at floor number No. 4 is reduced from 2.1 to 1.19 in loading No. EL1 and from 2.6 to 0.79 in loading No. EL2. According to above analysis and the previous work [27], the SSI effect should be considered in the seismic design of structure, which should be benefit to the anti-seismic of a non-isolated structure but go against the seismic performance of the isolation layer for a base-isolated structure.

3.5. Combined isolation of the soil foundation and the isolation layer

The above analyses demonstrate that the isolation efficiency of the isolation layer decreases as the PGA of the input motion increases. However, some previous studies have shown that a soft soil layer has a natural isolation ability during a strong earthquake [18,22]. Accordingly, Fig. 18 shows the AMFs of the SSI effect from the bedrock to the top of the isolated structure. Importantly, the seismic responses of the isolated structure exhibit a strongly decreasing trend as the PGA of the input motion increases, indicating that the natural isolation property of the soft soil layer can compensate for the lost isolation ability of the isolation layer. The main reason is that, though the isolation efficiency of the isolation layer was reduced by SSI effect, the input ground motion at the bottom of the base-isolated structure was also reduced greatly. This result demonstrates that the effect of SSI should be included in the seismic design of a base-isolated structure that is built on soft soil. As a result, the construction cost of the isolation layer should decrease, and the isolation layer may even be omitted if the natural isolation of the soft soil ground can satisfy the anti-seismic requirements of the non-isolated structure, as was also suggested by Chen et al. [5]. However, it should be stated that the soft soil layer may increase the dominant period of ground motions to be close to the nature period of the base-isolated structure, which may cause the structure resonance. In this point, how to take advantage of the natural isolation of the soft soil ground should be studied in deeply.

4. Conclusions

Shaking table tests were conducted to study the effect of SSI on the seismic responses of a base-isolated structure on a multi-layered soft soil. The seismic responses of the SSI system are analysed and compared with results of a previous study. The main findings from this study can be summarized as follows:

1. The spectrum characteristics of the input motion greatly influenced the isolation efficiency of an isolation layer on a soft soil. Generally, due to the earth-filtering effect, the low frequency vibration of the input motion is amplified by the softening clay layer. As a result, the predominant period of site should be closer to the natural period of base-isolated structure, and then the isolation efficiency of the isolation layer significantly decreases as the PGA of the input motion increases.
2. The rotation responses of the pile cap and the isolation layer are both more severe on a soft soil than on a harder soil. In particular, the rotation responses become stronger as the PGA of the input motion increases, which is contrary to the trend observed in previous model tests with a harder soil. However, the rotation vibration has not considered in the seismic design of a base-isolated structure, which should also affect the working condition of the lead-rubber bearing. How to control the rotation vibration of a base-isolated structure built on soft soil site should be studied in detail.
3. Generally, the rotation responses of the pile cap were greatly amplified by the isolation layer, which was also observed in previous model tests with a stiffer soil [27]. However, this amplifying effect mostly becomes stronger as the PGA of the input motion increases, which also differs from the results of the previous model test [27]. The reason for this discrepancy is that the low frequency vibrations of the input motion are amplified by the softening clay layer, which causes the predominant period of the soil foundation to be more similar to that of the base-isolated structure.
4. The acceleration responses at the middle floors of the isolated structure were smaller than those at the top and bottom floors, which is also found for the isolated structure on a rigid soil

foundation or stiffer soil foundation. However, as the PGA of the input motion increases, the floor number with the smallest acceleration changed within the middle floors of the isolated structure. The reason is that the predominant period of engineering site should be increased by the softening soil with the PGA of the input motion increasing, which should affect the acceleration responses of a base-isolated structure.

5. Under the combined isolation of the soft soil layer and the isolation layer, the seismic responses of the isolated structure decrease as the PGA of the input motion increases, which means that the natural isolation properties of the soft soil layer can compensate for the lost isolation ability of the isolation layer. Especially, the isolation layer may even be omitted if the natural isolation of the soft soil ground can be properly utilized in the seismic design of a non-isolated structure.
6. However, it should be stated that the soft soil layer may increase the dominant period of ground motions and thus be close to the nature period of the base-isolated structure, which may cause the structure resonance. Meanwhile, the isolation efficiency of isolation layer should be reduced by the soil foundation. How to take advantage of the natural isolation of the soft soil ground should be studied in deeply.

Acknowledgments

This research was funded by the National Natural Science Foundation of China (NSFC, Grant No. 51778290; 51778282) and the Natural Science Foundation of Jiangsu for high school, China (NSFJ, Grant No. 16KJA560001). This support is gratefully acknowledged. All the statements, results and conclusions are those of the authors and do not necessarily reflect the views of NSFC and NSFJ. The authors would also like to thank the anonymous reviewers for their comments and suggestions.

References

[1] Bo JS, Li XL, Liu HS. Effect of soil layer construction on peak accelerations of ground motions. Earthq Eng Eng Vibrat 2003;23(3):35–40.
[2] Chen GX, Wang ZH, Zuo X, et al. Shaking table test on the seismic failure characteristics of a subway station structure on liquefiable ground. Earthq Eng Struct Dyn 2013;42(10):1489–507.
[3] Chen GX, Chen S, Qi CZ, Du XL, et al. Shaking table tests on a three-arch type subway station structure in a liquefiable soil. Bull Earthq Eng 2015;12:1675–701.
[4] Chen KF, Zhang SW. Improvement on the damping estimation by half power point method. Chin J Vibrat Eng 2002;15(2):151–5.
[5] Chen YQ, Lv XL, Li PZ, et al. Effects of soil-structure interaction with various soils on foundation motion. Eng J Wuhan Univ 2005;38(3):63–8.
[6] Constantinou MC, Kneifati M. Dynamics of soil-base-isolation structure systems. J Struct Eng 1988;114(1):211–21.
[7] Hokmabadi AS, Behzad F, Samali BJ. Assessment of soil–pile–structure interaction influencing seismic response of mid-rise buildings sitting on floating pile foundations. Comput Geotech 2014;55:172–86.
[8] Japan Society of Civil Engineers (JSCE). Standard Specifications for Concrete Structures – 2002: Seismic Performance Verification. JSCE Guidelines for Concrete No. 5; 2005.
[10] Kokusho T. Seismic base-isolation mechanism in liquefied sand in terms of energy. Soil Dyn Earthquake Eng 2014;63:92–7.
[11] Li CP, Liu WQ, Wang SG, Du DS, Wang H. Shaking table test on high-rise isolated structure on soft soil foundation. J Build Struct 2013;34(7):72–8.
[12] Ling XZ, Wang C, Wang C. Scale modeling method of shaking table test of dynamic interaction of pile-soil-bridge structure in ground of soil liquefaction. Chin J Rock Mech Eng 2004;23(3):450–6.
[13] Luco JE. Effects of soil–structure interaction on seismic base isolation. Soil Dyn Earthq Eng 2014;66:167–77.
[14] Lv XL, Chen YQ. Study on dynamic similitude theory of soil-structure interactions system. Earthq Eng Eng Vibrat 2001;21(3):85–92.
[15] Mylonakis G, Gazetas G. Seismic soil structure interaction: beneficial or Detrimental? J Earthq Eng 2000;4(3):277–301.
[16] Mylonakis G, Gazetas G, Nikolaou S, Michaelides O. The role of soil on the collapse of 18 piers of the Hanshin expressway in the Kobe earthquake. Proceedings of 12th world conference on earthquake engineering, New Zealand, Paper No. 1074. 2000.
[17] Novak M, Hendreson P. Base-isolated building with soil-structure interaction. Earthq Eng Struct Dyn 1989;18(6):751–65.
[18] Pender MJ. Nonlinear cyclic soil-structure interaction. Pacific conference on earthquake engineering, Wairakei, New Zealand, vol. 3. 1987. p. 83–93.
[19] Sato N, Kato A, Fukushima Y, Iizuka M. Shaking table tests on failure characteristics of base isolation system for a DFBR plant. Nucl Eng Des 2002;212:293–305.
[20] Sayed M, Per-Erik A, Robert J. Non-linear behavior of base-isolated building supported on flexible soil under damaging earthquakes. Key Eng Mater 2012;488–489:142–5.
[21] Spyrakos CC, Maniatakis CA, Koutromanos IA. Soil-structure interaction effects on base-isolated buildings founded on soil stratum. Eng Struct 2009;31(3):729–37.
[22] Trifunac MD. Nonlinear soil response as a natural passive isolation mechanism. Paper II. The 19333 Long Beach, California earthquake. Soil Dyn Earthq Eng 2003;23(7):549–62.
[23] Wolf JP. Dynamic soil-structure interaction. Englewood Cliffs, New Jersey: Prentice-Hall Inc; 1985.
[24] Yasuda S, Ishihara K, Morimoto I, Orense R, et al. Large-scale shaking table tests on pile foundations in liquefied ground. Proc. 12th World Conf. Earthquake Eng New Zealand, Paper No. 1474. 2000.
[25] Yu X, Zhuang HY, Liu S. Simple method for the dynamic responses of soil-pile-isolated structure interaction system. Trans Nanjing Univ Aeronaut Astronaut 2017;34(4):405–12.
[26] Yuan Y, Zhu K, Xiong SS, et al. Experimental study on characteristics and isolator effect of high-damping rubber bearing. Earthq Resist Eng and Retrofit 2008;30(3):15–20.
[27] Zhuang HY, Yu X, Zhu C, Jin DD. Shaking table tests for the seismic response of a base-isolated structure with the SSI effect. Soil Dyn Earthq Eng 2014;67(6):208–18.
[28] Zhuang HY, Hu ZH, Wang XJ, Chen GX. Seismic responses of a large underground structure in liquefied soils by FEM numerical modelling. Bull Earthq Eng 2015;13(12):3645–68.
[29] Zhuang HY, Chen GX, Hu ZH, Qi CZ. Influence of soil liquefaction on the Seismic response of a subway station by the model tests. Bull Eng Geol Environ 2016;75(4):1169–82.